Journal of Coordination Chemistry
Publication details, including instructions for authors and subscription information:
http://www.tandfonline.com/loi/gcoo20

Synthesis, structure, cytotoxic activities, and DNA-binding of 1-D copper(II) and zinc(II) coordination polymers

Man Jiang [a b], Yan-Tuan Li [a] & Zhi-Yong Wu [a]

[a] Marine Drug & Food Institute, Ocean University of China, 5 Yushan Road, Qingdao, Shandong 266003, P.R. China

[b] Qindao Municipal Medical Group, Qindao, Shandong 266011, P.R. China

Published online: 08 May 2012.

To cite this article: Man Jiang, Yan-Tuan Li & Zhi-Yong Wu (2012) Synthesis, structure, cytotoxic activities, and DNA-binding of 1-D copper(II) and zinc(II) coordination polymers, Journal of Coordination Chemistry, 65:11, 1858-1871, DOI: 10.1080/00958972.2012.680591

To link to this article: http://dx.doi.org/10.1080/00958972.2012.680591

Journal of Coordination Chemistry
Vol. 65, No. 11, 10 June 2012, 1858–1871

Synthesis, structure, cytotoxic activities, and DNA-binding of 1-D copper(II) and zinc(II) coordination polymers

MAN JIANG†‡, YAN-TUAN LI*† and ZHI-YONG WU†

†Marine Drug & Food Institute, Ocean University of China, 5 Yushan Road, Qingdao, Shandong 266003, P.R. China
‡Qindao Municipal Medical Group, Qindao, Shandong 266011, P.R. China

(*Received 8 September 2011; in final form 28 February 2012*)

Two 1-D coordination polymers have been synthesized and identified as $[Zn(ox)(en)]_n(H_2O)_{2n}$ (**1**) and $[Cu_2(dmeo)(N_3)_2]_n$ (**2**), where en represents diaminoethane, ox and dmeo stand for dianions of oxalic acid and *N*,*N*′-bis[2-(dimethylamino)ethyl]oxamide, respectively. Polymer **1** was characterized by elemental analysis, molar conductance measurement, IR and electronic spectra, and single-crystal X-ray diffraction. Polymer **1** consists of 1-D chains bridged by oxalate. The Zn^{II} can be described as a distorted octahedral environment and the $Zn^{II}\cdots Zn^{II}$ separation through the μ-oxalato-bridge is 5.5420(9) Å. Hydrogen bonds assemble the coordination polymers to a 3-D supermolecular structure. The crystal structure of **2** has been reported previously. However, the bioactivities were not studied. The DNA-binding properties and cytotoxic activities of the two coordination polymers are investigated. The results suggest that the two polymers interact with *HS*-DNA in groove binding with binding affinity following the order of **1** > **2**, which is consistent with their anticancer activities.

Keywords: Crystal structure; 1-D coordination polymers; Copper(II); Zinc(II); DNA interaction; μ-Oxamido-bridge; μ-Oxalate-bridge

1. Introduction

The design, synthesis, and interaction of DNA with transition metal complexes have been active fields of research, not only for theoretical interest to elucidate the mechanism involved in the site specific recognition of DNA and to determine the principles governing the recognition, but also for understanding models for protein–nucleic acid interactions, application of probes of DNA structure, and the exploitation of the synthesis of new types of pharmaceutical molecules [1–7]. Modes of DNA noncovalent interaction with metal complexes include electrostatic effect, groove binding, and intercalation; effectiveness mainly depends on the mode and affinity of the binding between the complexes and DNA [8, 9]. Many transition metal complexes have been synthesized and their interactions with DNA are studied [10–20]. Significant developments have occurred in the chemistry of polymer–metal complexes.

*Corresponding author. Email: yantuanli@ouc.edu.cn

ISSN 0095-8972 print/ISSN 1029-0389 online
http://dx.doi.org/10.1080/00958972.2012.680591

In particular, studies on the interaction of polymer–metal complexes with DNA have been of great interest [21, 22]. However, examples of such polymer–metal complexes are still few and comparatively little attention has been given to systems in which the transition metal ions are propagated by oxamide or oxalate bridges, although oxamide and oxalate have been shown to be excellent bridges for constructing polymer–metal complexes [23, 24]. Thus, it is of considerable interest to synthesize and study the DNA-binding properties of polymer–metal complexes with bridging oxamide and oxalate groups in order to gain insight into the DNA-binding properties and antitumor activities of these kinds of complexes.

In this article, two 1-D coordination polymers have been synthesized and characterized as $[Zn(ox)(en)]_n(H_2O)_{2n}$ (**1**) and $[Cu_2(dmeo)(N_3)_2]_n$ (**2**), where en represents diamino-ethane, ox and dmeo stand for the dianions of oxalic acid and *N*,*N*′-bis[2-(dimethylamino)ethyl]oxamide, respectively. The cytotoxicities reveal that both polymer–metal complexes exhibit potent cytotoxic effects against human hepatocellular carcinoma SMMC-7721 and human lung adenocarcinoma A549. Interaction of the two coordination polymers with herring sperm DNA (*HS*-DNA) was investigated by using electronic absorption spectroscopy, fluorescence spectroscopy, and viscosity measurements; the results suggest that the two polymers interact with *HS*-DNA through groove binding and their DNA-binding abilities are consistent with *in vitro* antitumor activities, following the order **1** > **2**.

2. Experimental

2.1. *Materials*

N,*N*′-bis[2-(dimethylamino)ethyl]oxamide and **2** were synthesized according to the reported methods [25, 26]. Ethidium bromide (EB) and *HS*-DNA were purchased from Sigma Corp. and used as received. All other reagents were of analytical grade.

2.2. *Synthesis of* $[Zn(ox)(en)]_n(H_2O)_{2n}$ *(1)*

To a solution of $Zn(ClO_4)_2 \cdot 6H_2O$ (74.4 mg, 0.2 mmol) stirred in water (5 mL), a methanol solution (5 mL) of en (12.0 mg, 0.2 mmol) was added dropwise at room temperature. The vigorous stirring was continued until the mixture became limpid (about 30 min). It was then filtered to eliminate impurities. A water solution (10 mL) of potassium oxalate monohydrate (36.9 mg, 0.2 mmol) was slowly added to the filtrate (containing $[Zn(en)(H_2O)_4]^{2+}$ precursor) with rapid stirring at room temperature. The color of the solution turned from blue to light-green immediately. After refluxing for *ca* 2 h, the resulting solution was then allowed to cool to room temperature and green-cube crystals of the coordination polymer suitable for the X-ray analysis were obtained by slow evaporation at room temperature. Yield: 65%. Anal. Calcd for $ZnC_4H_{12}N_2O_6$ (%): C, 19.25; H, 4.85; N, 11.23; Zn, 26.21. Found (%): C, 19.23; H, 4.82; N, 11.27; Zn, 26.10.

2.3. *Physical measurements*

The C, H, and N microanalyses were performed on a Perkin-Elmer 240 elemental analyzer. Metal contents were determined on an ICP-4300 isoionic emission spectrophotometer. Infrared (IR) spectra were recorded on a Nicolet-470 spectrophotometer from 4000 to 400 cm^{-1} as KBr pellets. Electronic spectra were measured on a Cary 300 spectrophotometer and fluorescence spectra were measured with an Fp-750w Fluorometer. Viscosity measurement was carried out using an Ubbelodhe viscometer immersed in a thermostatic water bath maintained at 289(±0.1) K. Cyclic voltammetric experiments were carried out using a CHI 832B electrochemical analyzer in connection with a glassy carbon working electrode, saturated calomel reference, and a platinum wire auxiliary electrode.

2.4. *Crystal structure determination*

The X-ray diffraction measurements for **1** were carried out on a Bruker SMART CCD diffractometer using graphite monochromated Mo-Kα radiation ($\lambda = 0.71073$ Å) at 293 K. Parameters of the unit cell were refined by SAINT with 20 reflections in the range $5.1^\circ < 2\theta < 12.8^\circ$. Data were collected by SMART in a ω and ψ scan and reduced by SAINT. Intensities of three standard reflections were measured for every 100 reflections. Absorption corrections were applied by multi-scan. The structures were solved by the SIR-97 program. Structure refinement was carried out using the SHELXL-97 program [27]. All non-hydrogen atoms were refined anisotropically by the full-matrix least-squares method. The carbons of en in **1** are disordered in two positions with site occupancy factors of 0.7 and 0.3, respectively. Hydrogen atoms of water were located in a difference Fourier map and others were placed in calculated positions; all hydrogen atoms were included in the structure-factor calculations with fixed coordinates and isotropic displacement parameters of 0.08 Å. Crystal data and structural refinement parameters for **1** are summarized in table 1. Selected bond distances and angles are listed in tables 2 and 3.

2.5. In vitro *antitumor activity evaluation by SRB assays*

In vitro antitumor activities of the two polymers and *cis*-platin were evaluated against two cancer cell lines including SMMC-7721 and A549 by using the Sulforhodamine B (SRB) assay. All cells were cultured in RPMI 1640 supplemented with 10% (v/v) fetal boving serum, 1% (w/v) penicillin (104 U mL^{-1}), and 10 mg mL^{-1} streptomycin. Cell lines are maintained at 310 K in a 5% (v/v) CO_2 atmosphere with 95% (v/v) humidity. Cultures were passaged weekly using trypsin-EDTA to detach the cells from their culture flasks. The two polymers were dissolved in DMSO and diluted to the required concentration with culture medium when used. The content of DMSO in the final concentrations did not exceed 0.1%. At this concentration, DMSO was found to be non-toxic to the cells tested. Rapidly growing cells were harvested, counted, and incubated at the appropriate concentration in 96-well microplates for 24 h. The two polymers dissolved in culture medium were then applied to the culture wells to achieve final concentrations ranging from 10^{-4} to 10^{2} μg mL^{-1}. Control wells were prepared by the addition of culture medium without cells. The plates were incubated at 310 K in a

Table 1. Summary of crystallographic data for **1**.

Empirical formula	$C_4H_{12}N_2O_6Zn$
Formula weight	249.53
Wavelength (Å)	0.71073
Crystal system	Monoclinic
Space group unit cell dimensions (Å,°)	*C*2/*c*
a	11.9488(16)
b	9.0492(10)
c	9.272(2)
β	114.898(14)
Volume (Å^3), *Z*	909.3(3), 4
Calculated density (g cm^{-3})	1.823
Absorption coefficient (mm^{-1})	2.704
F(000)	512
Crystal size (mm^3)	0.22 × 0.24 × 0.33
θ range for data collection (°)	2.93–30.98
Limiting indices	$-17 \le h \le 1$; $0 \le k \le 13$; $-12 \le l \le 13$
Reflections collected	1626
Independent reflections	1445 [R(int) = 0.0215]
Completeness to $\theta = 30.98$ (%)	99.8
Data/restraints/parameters	1445/0/69
Goodness-of-fit on F^2	1.056
Final *R* indices [$I > 2\sigma(I)$]	$R_1 = 0.0302$, $wR_2 = 0.0695$
R indices (all data)	$R_1 = 0.0394$, $wR_2 = 0.07233$
Largest difference peak and hole (e Å^{-3})	0.346 and −0.372

Table 2. Selected bond distance (Å) and angles (°) for **1**.

Zn–N1	2.1143(19)	Zn–O1	2.1169(14)
Zn–O2^{iii}	2.1443(14)	N1–C2A	1.481(5)
C2A–C2A^{i}	1.522(10)	N1–C2B	1.526(10)
C2B–C2B^{i}	1.45(2)	C1–O1	1.252(2)
C1–O2	1.249(2)	C1–C1^{ii}	1.559(4)
N1–Zn–N1^{i}	83.33(11)	O1–Zn–O2^{iii}	91.49(6)
O1–Zn–O1^{i}	165.70(8)		
Zn–N1–C2A–C2A^{i}	46.2(5)	Zn–N1–C2B–C2B^{i}	−41.3(12)
N1–C2A–C2A^{i}–N1^{i}	−63.8(7)	N1–C2B–C2B^{i}–N1^{i}	55.9(16)

Symmetry codes: (i) = $-x$, y, $-z+1/2$; (ii) = $-x$, $-y+1$, $-z$; (iii) = x, $-y+1$, $-z+1/2$.

Table 3. Hydrogen-bonding geometry (Å and °).

D–H···A	*d*(D–H)	*d*(H···A)	*d*(D···A)	∠(DHA)
N1–H1B···O1W	0.906(2)	2.400(2)	3.237(3)	153.71(13)
O1W–H2W···O1	0.8272(18)	2.0685(14)	2.761(2)	141.01(18)
N1–H1A···O1W^{iv}	0.905(2)	2.269(2)	3.147(3)	163.72(13)
O1W–H1W···O2^{v}	0.8949(19)	2.0065(14)	2.888(2)	167.98(12)

Symmetry codes: (iv) = $-x+1/2$, $-y+1/2$, $-z+1$; (v) = $-x+1/2$, $-y+1/2$, $-z$.

5% CO_2 atmosphere for 48 h. Upon completion of the incubation, the cells were fixed with ice-cold 10% trichloroacetic acid (100 mL) for 1 h at 277 K, washed five times in distilled water and allowed to dry in air, and stained with 0.4% SRB in 1% acetic acid (100 mL) for 15 min. The cells were washed four times in 1% acetic acid and air-dried. The stain was solubilized in 10 mmol L^{-1} unbuffered Tris base (100 mL) and the OD of each well was measured at 540 nm on a microplate spectrophotometer. The IC_{50} values were calculated from the curves constructed by plotting cell survival (%) *versus* the polymers concentration (μg mL^{-1}).

2.6. *DNA-binding studies*

All experiments involving *HS*-DNA were performed in Tris-HCl buffer solution (pH = 7.12). Tris-HCl buffer was prepared using deionized and sonicated triply-distilled water. Solutions of *HS*-DNA in Tris-HCl gave a ratio of UV absorbance at 260 and 280 nm, A_{260}/A_{280}, of *ca* 1.9, indicating that the DNA was sufficiently free from protein [28]. The concentration of *HS*-DNA was determined by UV absorbance at 260 nm. The extinction coefficient, $\varepsilon 260$, was taken as 6600 L mol^{-1} cm^{-1} [29]. Stock solution of *HS*-DNA was stored at 277 K and used after no more than 4 days. Concentrated stock solution of the two polymers were prepared by dissolving the complexes in DMSO and diluted suitably with Tris-HCl buffer to required concentrations for the experiments. Absorption spectral titration experiments were performed by keeping the concentration of the polymers constant while varying the *HS*-DNA concentration. Equal solution of *HS*-DNA was added to the polymer solution and reference solution to eliminate the absorbance of DNA itself. In the EB fluorescence displacement experiment, 5 μL of the EB Tris-HCl solution (1 mmol L^{-1}) was added to 1 mL of *HS*-DNA solution (at saturated binding levels [30]) and stored in the dark for 2 h. The solution of the polymer was titrated into the *HS*-DNA/EB mixture and then diluted in Tris-HCl buffer to 5 mL, producing solutions with varied mole ratio of the polymer to *HS*-DNA. Before measurements, the mixture was shaken and incubated at room temperature for 30 min. The fluorescence spectra were obtained at an excitation wavelength of 522 nm and an emission wavelength of 584 nm in the fluorometer. Viscosity measurements were performed using an Ubbelodhe viscometer immersed in a thermostatic water bath maintained at 289(±0.1) K. DNA samples approximately 200 base pairs in length were prepared by sonication in order to minimize complexities arising from DNA flexibility [31]. Flow times were measured with a digital stopwatch, each sample was measured thrice, and an average flow time was calculated. Relative viscosities for *HS*-DNA in the presence and absence of the complexes were calculated from the relation $= (t - t_0)/t_0$, where t is the observed flow time of *HS*-DNA-containing solution and t_0 is that of Tris-HCl buffer alone. Data were presented as $(\eta/\eta_0)^{1/3}$ *versus* [complex]/[DNA] [32], where is the viscosity of *HS*-DNA in the presence of the polymers and $_0$ is that of *HS*-DNA alone.

3. Results and discussion

3.1. *Synthesis and general characterization of polymer 1*

A polymorph of polymer **1** was previously obtained by 2,2′-biimidazoline hydrolysis to give ethylenediamine molecules and oxalate anions [33]. In this study, compound **1**,

prepared by the treatment of $Zn(ClO)_2 \cdot 6H_2O$ with ethylenediamine (en) and potassium oxalate in aqueous methanol, belongs to the general class of oxalato-bridged, 1-D zinc(II) coordination polymers of formulation **1**. Polymer **1** is soluble in DMF, DMSO, methanol, and water to give stable solutions at room temperature; it is moderately soluble in ethanol, acetone, and acetonitrile, and practically insoluble in carbon tetrachloride, chloroform, and benzene. In the solid state, **1** is sufficiently stable in air to allow physical measurements. For **1**, the molar conductance value in DMF solution ($10\ \Omega^{-1}\,cm^{-2}\,mol^{-1}$) falls in the expected range for non-electrolytes [34], in agreement with single-crystal X-ray structure analysis. In the IR spectrum of **1**, bridging oxalate is clearly observed in the stretching and deformation, ν_{as}(O–C–O) at $1640\,cm^{-1}$, ν_s(O–C–O) at $1350\,cm^{-1}$, and δ(O–C–O) at $728\,cm^{-1}$ attributed to bischelating oxalate [35, 36]. The $\nu(NH_2)$ at $3250\,cm^{-1}$ stretching vibration of the end-capping en is found in **1**, suggesting that en coordinates with zinc(II). The electronic spectrum of the polymer was measured in DMSO solution. A band centered at 265 nm may be attributed to metal-to-ligand charge transfer.

3.2. *Crystal structure*

Since the structure of **2** has already been reported [26], the discussion here is focused on the structure of **1**. The crystal structure of **1** is shown in figure 1 and the selected bond distances and angles are illustrated in table 2.

As shown in figure 1, the asymmetric unit of **1** contains half of the [Zn(ox)(en)] complex fragment and one solvent water. There is an inversion center at the middle of

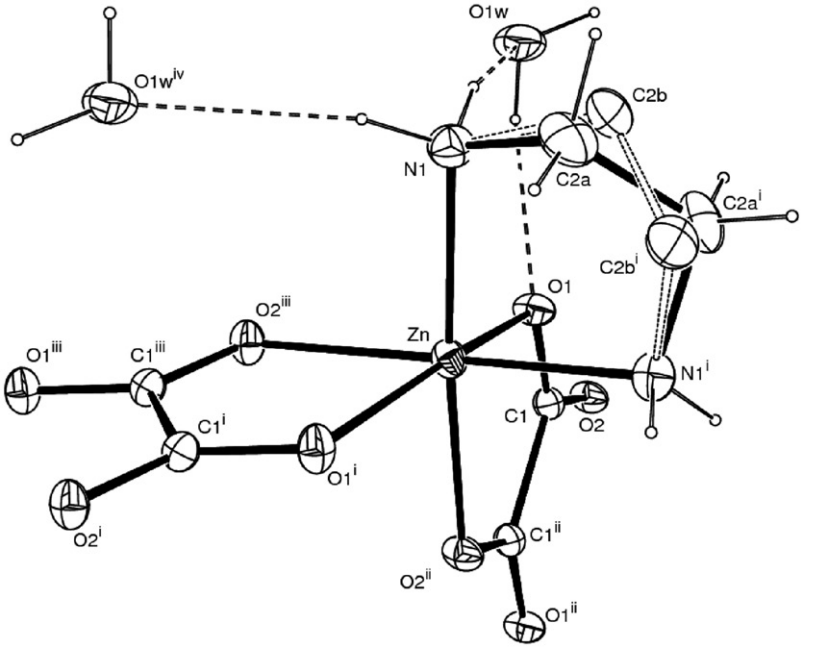

Figure 1. ORTEP drawing of $[Zn(ox)(en)]_n(H_2O)_{2n}$ with 30% probability displacement ellipsoids (symmetry codes: (i) $= -x, y, -z+1/2$; (ii) $= -x, -y+1, -z$; (iii) $= x, -y+1, -z+1/2$; (iv) $= -x+1/2, -y+1/2, -z+1$).

the carbon atoms [C1 and C1^{ii}, symmetry code: (ii) $= -x, -y+1, -z$] of oxalate. A two-fold rotation axis passes through zinc(II) and the center of the two carbon atoms of ethylenediamine. Zinc(II) has a slightly distorted $\{O_4N_2\}$ octahedral environment constructed by one ethylenediamine and two oxalate anions in a *cis*-arrangement. The equatorial plane is formed by N1 and N1^{i} [symmetry code: (i) $= -x, y, -z+1/2$] from an ethylenediamine and two carboxyl oxygen atoms [O2^{ii} and O2^{iii}, symmetry code: (iii) $= x, -y+1, -z+1/2$] from two adjacent oxalate anions. The axial positions are occupied by two other carboxyl oxygen atoms [O1 and O1^{i}] from the two oxalate anions. The deviations from the least-squares plane of the equatorial plane vary within 0.0963(12) and 0.1016(13) Å.

Tetradentate oxalate anions bridge the $[Zn(en)]^{2+}$ fragments (figure 2) as a μ^2-ligand [37] to form a zig-zag complex chain parallel to the *c*-axis with Zn $\cdots$ Zn separation of 5.5420(9) Å. The oxalate and ethylenediamine chelate to zinc(II) with bite angles of 91.49(6)° and 83.33(11)°, respectively. The carbon of ethylenediamine is disordered at two positions; both corresponding five-membered chelate rings are in a twist conformation.

In the crystal, due to the hydrogen bonds of water with ethylenediamine and oxalate (table 3, figure 3), the complex chains are assembled to a 3-D supramolecular structure, as revealed by figure 4.

The previously reported polymorph [33] of **1** exhibits a similar zig-zag complex chain to the one observed here. Although both compounds crystallize in the same $C2/c$ space group, the volume of the cell of the reported polymorph [2706.4(11) Å^3, $a = 25.757(5)$ Å, $b = 9.053(3)$ Å, $c = 11.623(2)$ Å, $\beta = 93.05(3)°$] is almost three times that of **1** [909.3(3) Å^3]. The reported polymorph has a lower symmetry than polymer **1**. The previously reported polymorph of **1** contains one and a half Zn(II) ions and one and a half oxalate anions in the asymmetric unit. Thereby, for the reported polymorph there are two kinds of Zn(II), oxalate, and ethylenediamine in different environments, which contribute to the larger crystal cell.

3.3. In vitro *antitumor activities of the coordination polymers*

In vitro antitumor activities of **1**, **2**, and *cis*-platin against two cancer cell lines, human hepatocellular carcinoma SMMC-7721 and human lung adenocarcinoma A549, were

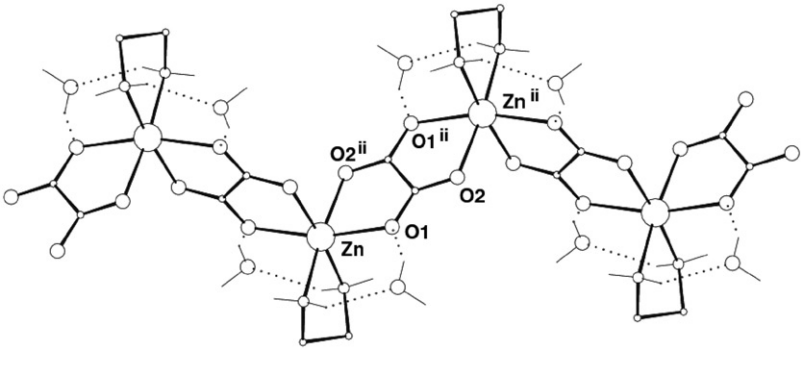

Figure 2. The zig-zag arrangement along the *c*-axis of $[Zn(ox)(en)]_n(H_2O)_{2n}$. (Symmetry codes: (ii) $= x, -y+1, -z$).

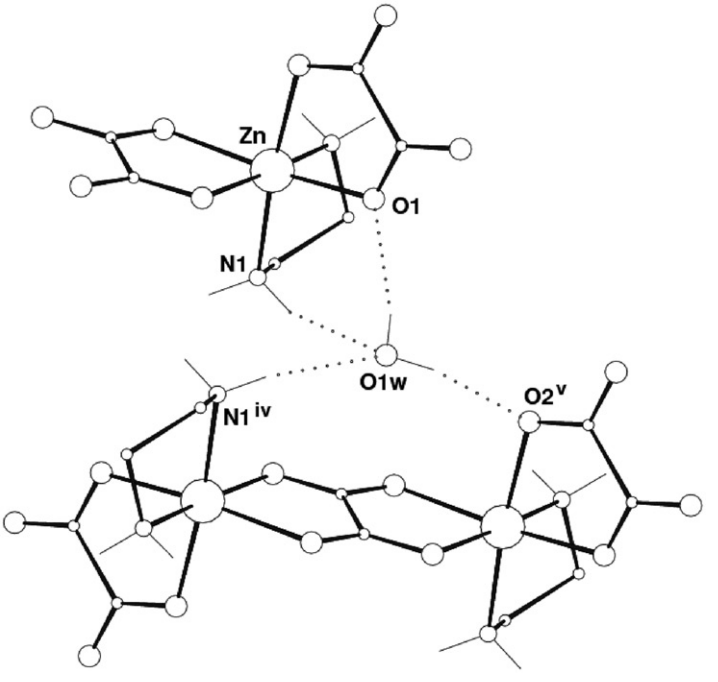

Figure 3. The crystal water connecting the $[Zn(ox)(en)]_n(H_2O)_{2n}$ by hydrogen bonds. (Symmetry codes: (iv) $= -x+1/2, -y+1/2, -z+1$; (v) $= -x+1/2, -y+1/2, -z$).

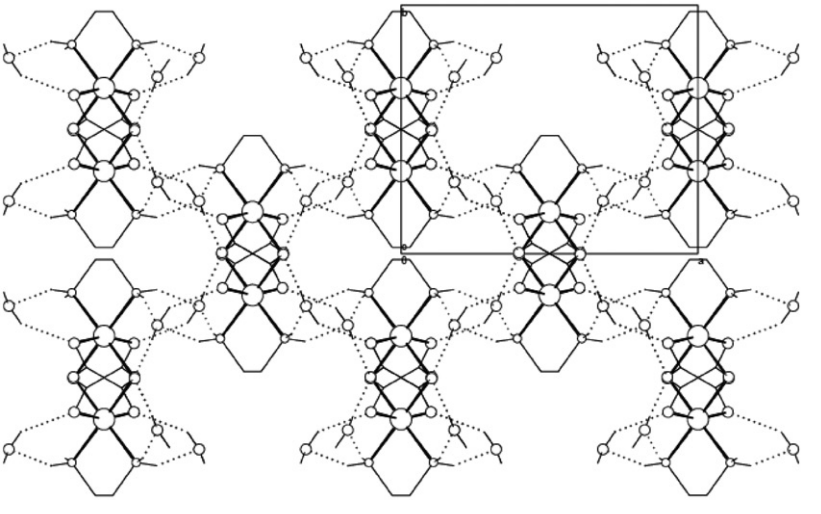

Figure 4. A 3-D supermolecular structure of $[Zn(ox)(en)]_n(H_2O)_{2n}$ assembled by hydrogen bonds.

measured in our study. As shown in table 4, the two polymers have cytotoxicities against the two cancer cell lines and **1** showed better activity than **2**. Although the measured cytotoxic activity is less than that of *cis*-platin, inhibition of cell proliferation produced by the two polymers on the same batch of cell lines and under identical

Table 4. *In vitro* antitumor activities of the polymers and *cis*-platin against human hepato-cellular carcinoma cell line SMMC-7721 and human lung adenocarcinoma cell A549.

	IC_{50} ($\mu g\,mL^{-1}$)	
Complexes	SMMC-7721	A549
$[Zn(ox)(en)]_n(H_2O)_{2n}$ (**1**)	8.2 ± 1.6	5.0 ± 1.1
$[Cu_2(dmeo)(N_3)_2]_n$ (**2**)	14.9 ± 1.2	10.5 ± 1.8
Cis-platin	$5.4 \pm 0.2\,ng\,mL^{-1}$	$7.6 \pm 0.4\,ng\,mL^{-1}$

experimental conditions is still rather active, with IC_{50} values falling in the 5–15 $\mu g\,mL^{-1}$ range. These cytotoxic activities *in vitro* prompted us to explore DNA-binding of the two polymers.

3.4. *DNA-binding studies*

3.4.1. Electronic absorption titration. Electronic absorption spectroscopy is one of the most useful techniques for DNA-binding studies of metal complexes. The electronic spectra of the two polymers in the presence and absence of *HS*-DNA are illustrated in figure 5. Addition of *HS*-DNA results in a hyperchromism in absorption intensity, indicating that there exists an interaction between the two polymers and *HS*-DNA, which is different from classical intercalation. These spectral features are analogous to that of our previously reported 2-D copper(II) polymer $[Cu_4(H_2O)_4(dmapox)_2(btc)]_n \cdot 10nH_2O$ [21], whose interaction mode with DNA is groove binding. Therefore, the present observation leads us to suspect that the two polymers are groove binding, leading to small perturbations.

To quantitatively evaluate the binding magnitude of the two polymers with *HS*-DNA, the intrinsic binding constants (K_b) were determined by monitoring the changes in absorbance at 265 and 275 nm for **1** and **2**, respectively, using the following equation [38]:

$$[DNA]/(\varepsilon_a - \varepsilon_f) = [DNA]/(\varepsilon_b - \varepsilon_f) + 1/K_b(\varepsilon_b - \varepsilon_f) \quad (1)$$

where ε_f, ε_a, and ε_b correspond to the extinction coefficients, respectively, for the free polymer, for each addition of DNA to the polymer, and for the polymer in the fully bound form. The ratio of the slope to the intercept in the plot of $[DNA]/(\varepsilon_a - \varepsilon_f)$ *versus* [DNA] (figure 5) gives values of K_b as $6.88 \times 10^4\,mol\,L^{-1}$ ($R^2 = 0.9986$ for six points) for **1** and $7.62 \times 10^3\,mol\,L^{-1}$ ($R^2 = 0.9971$ for eight points) for **2**. The binding ability of the two polymers to *HS*-DNA follows the order **1** > **2**, indicating that **1** interacts with *HS*-DNA more strongly than **2**. Comparing the structures of the two polymers, both consist of zig-zag chains, while methyl incorporated into the bridging ligand in **2** may cause hindrance when the polymer interacts with *HS*-DNA [39]. Additionally, the electron-pushing substituent ($-CH_3$) may increase the charge density of **2** and decrease the binding affinity between the polymer and DNA. According to these results we deduce that the steric hindrance of the structures of polymers and the electronic effects

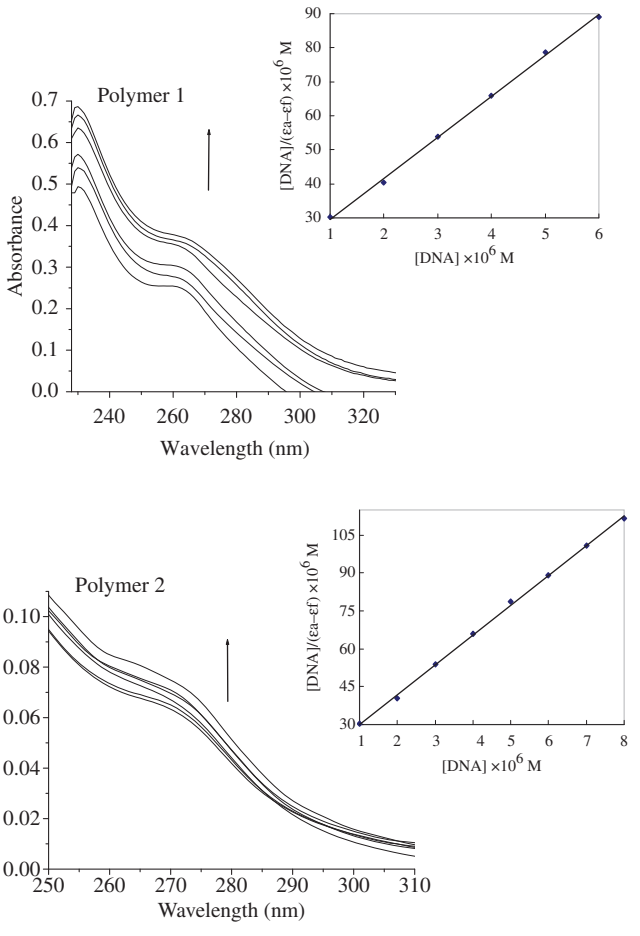

Figure 5. Electronic absorption spectra of $[Zn(ox)(en)]_n(H_2O)_{2n}$ (**1**) and $[Cu_2(dmeo)(N_3)]_n$ (**2**) upon the titration of *HS*-DNA. Inset: Plot of $[DNA]/(\varepsilon_a-\varepsilon_f)$ *vs.* [DNA] for the absorption titration of *HS*-DNA with the two polymers. Arrow indicates the direction of change upon increase of the DNA concentration.

of the ligand have a profound effect on DNA-binding, as revealed by the different binding affinities.

3.4.2. Fluorescence titration. The EB fluorescence displacement experiment has been widely used to investigate the interaction of metal complexes with DNA. In order to further investigate the interaction modes of the two polymers with *HS*-DNA, EB fluorescence displacement experiments were used. It is well known that EB is one of the most sensitive fluorescence probes that can bind with DNA. The fluorescence intensity of EB tends to increase after adding DNA due to intercalation into DNA. If the complex can intercalate into DNA, it will lead to decrease in the binding sites of DNA available for EB, and hence quenching of fluorescence intensity of EB-DNA mixture. Groove binding of the complex may also lead to quenching of EB emission [40]. As illustrated in figure 6, the fluorescence intensities of EB bound to *HS*-DNA at 584 nm

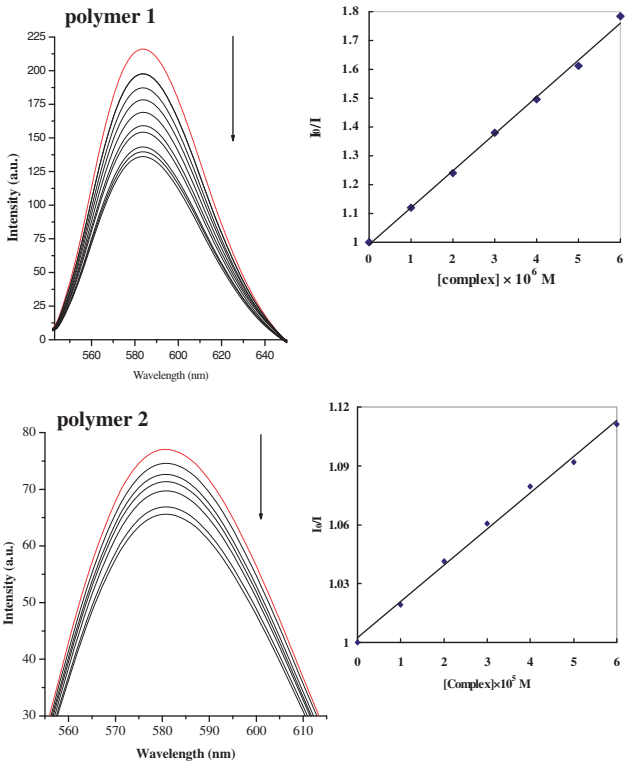

Figure 6. Fluorescence changes that occur when the *HS*-DNA-EB system is titrated with the polymers. Arrows show the intensity change upon increasing polymeric complex concentrations. Inset: Plot of I_0/I *vs.* [polymer] for the titration of the polymers to *HS*-DAN-EB system.

show remarkable decrease with increasing concentration of the two polymers, indicating that some EB molecules were released into the solution after exchange with the two polymers, which result in fluorescence quenching of EB.

To quantify the magnitude of the binding strength of the two polymers with *HS*-DNA, the linear Stern–Volmer equation is employed [41]:

$$I_0/I = 1 + K_{sv}[Q] \tag{2}$$

where I_0 and I represent the fluorescence intensities in the absence and presence of quencher, respectively. K_{sv} is a linear Stern–Volmer quenching constant and Q is the concentration of quencher. In the quenching plot (inset in figure 6) of I_0/I *versus* [complex], K_{sv} is given by the ratio of the slope to intercept. The K_{sv} values for the polymers are 1.29×10^5 ($R^2 = 0.9977$ for seven points) for **1** and 1.85×10^3 ($R^2 = 0.9955$ for seven points) for **2**; once again the binding ability of the two polymers to *HS*-DNA follows the order **1** > **2**.

3.4.3. Viscosity measurements. To further clarify the interactions of the polymers and *HS*-DNA, viscosity measurements were carried out. Viscosity measurement is sensitive to the changes in the length of DNA molecule and is regarded as the least ambiguous

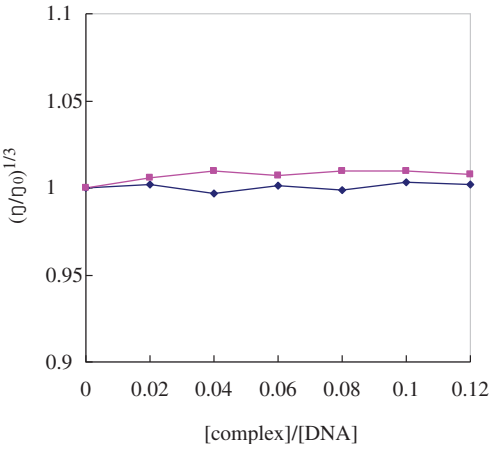

Figure 7. Effect of increasing amounts of the polymers (■ for **1** and ◆ for **2**) on the relative viscosity of *HS*-DNA at 289(±0.1) K, [DNA] = 0.2 mmol L^{-1}.

and most critical means studying the binding mode of metal complexes with DNA in solution [42, 43]. Intercalation of complexes to DNA causes a significant increase in the viscosity of a DNA solution due to the separation of the base pairs at the intercalation site and, hence, an increase in the overall DNA molecular length. However, in groove binding the length of the helix is unchanged resulting in no apparent alteration in DNA viscosity [44]. The effect of the two polymers on the viscosity of *HS*-DNA is shown in figure 7. The relative viscosity of *HS*-DNA remains essentially unchanged on addition of the polymers, very similar to that observed for our previously reported $[Cu_2(heae)(SCN)_2]_n \cdot nH_2O$ [45], which interacted with DNA in groove binding mode. Thus, the viscosity measurement is consistent with the results of the electronic absorption titration and EB fluorescence displacement experiments.

From the electronic absorption titrations, EB fluorescence displacement experiments, and viscometry measurements, and considering the non-planarity of the ligands in the two polymers, as well as the lack of change, one can conclude that groove binding is the most probable interaction between the two polymers and *HS*-DNA. Further investigations by using other methods to get a reasonable explanation and deeper insight into the DNA-binding mode of the polymers are in progress in our laboratory.

4. Conclusions

To investigate the influence of structural variation of the 1-D polymers on antitumor activities and DNA-binding properties, we synthesize two 1-D polymers $[Zn(ox)(en)]_n(H_2O)_{2n}$ (**1**) and $[Cu_2(dmeo)(N_3)_2]_n$ (**2**), where ox and dmeo stand for the dianions of oxalic acid and *N*,*N*′-bis[2-(dimethylamino)ethyl]oxamide, respectively. DNA-binding abilities of the two polymers are consistent with *in vitro* antitumor activities, following the order **1** > **2**, which suggest that the structural changes in polymers like the different substituent groups could influence their activities. These results should be valuable in understanding the interaction between polymers

and DNA, and laying a foundation for rational design of powerful agents for probing and targeting nucleic acids.

Supplementary material

Crystallographic data (excluding structure factors) for the new structure reported in this work (polymer **1**) have been deposited at the Cambridge Crystallographic Data Center and allocated the deposition number CCDC 841784.

Acknowledgments

This project was supported by the National Natural Science Foundation of China (No. 21071133) and the Program for Changjiang Scholars and Innovative Research Team in University (IRT0944).

References

[1] E.R. Jamieson, S.J. Lippard. *Chem. Rev.*, **99**, 2467 (1999).
[2] M. Mrksich, P.B. Dervan. *J. Am. Chem. Soc.*, **117**, 3325 (1995).
[3] K.E. Erkkila, D.T. Odom, J.K. Barton. *Chem. Rev.*, **99**, 2777 (1999).
[4] M.J. Clarke. *Coord. Chem. Rev.*, **236**, 209 (2003).
[5] H.T. Chifotides, K.R. Dunbar. *Acc. Chem. Res.*, **38**, 146 (2005).
[6] P.T. Selvi, H. Stoeckli-Evans, M.J. Palaniandavar. *Inorg. Biochem.*, **99**, 2110 (2005).
[7] V. Rajendiran, R. Karthik, M. Palaniandavar, H. Stoeckli-Evans, V.S. Periasamy, M.A. Akbarsha, B.S. Srinag, H. Krishnamurthy. *Inorg. Chem.*, **46**, 8208 (2007).
[8] P.M. Bradley, A.M. Angeles-Boza, K.R. Dunbar, C. Turro. *Inorg. Chem.*, **43**, 2450 (2004).
[9] R. Senthil Kumar, K. Sasikala, S. Arunachalam. *J. Inorg. Biochem.*, **102**, 234 (2008).
[10] E.L. Hegg, J.N. Burstyn. *Coord. Chem. Rev.*, **173**, 133 (1998).
[11] D.S. Sigman, T.W. Bruce, C.L. Sutton. *Acc. Chem. Res.*, **26**, 98 (1993).
[12] W.K. Pogozelski, T.D. Tullius. *Chem. Rev.*, **98**, 1089 (1998).
[13] D.S. Sigman, A. Mazumder, D.M. Perrin. *Chem. Rev.*, **93**, 2295 (1993).
[14] K.J. Humphreys, K.D. Karlin, S.E. Rokita. *J. Am. Chem. Soc.*, **123**, 5588 (2001).
[15] K.J. Humphreys, K.D. Karlin, S.E. Rokita. *J. Am. Chem. Soc.*, **124**, 6009 (2002).
[16] K.J. Humphreys, K.D. Karlin, S.E. Rokita. *J. Am. Chem. Soc.*, **124**, 8055 (2002).
[17] M. González-Álvarez, G. Alzuet, J. Borrás, B. Macías, A. Castiairas. *Inorg. Chem.*, **42**, 2992 (2003).
[18] Y.P. Li, Y.B. Wu, J. Zhao, P. Yang. *J. Inorg. Biochem.*, **101**, 28 (2007).
[19] K. Dhara, P. Roy, J. Ratha, M. Manassero, P. Banerjee. *Polyhedron*, **26**, 4509 (2007).
[20] R. Rao, A.K. Patra, P.R. Chetana. *Polyhedron*, **27**, 1343 (2008).
[21] Z.Q. Liu, Y.T. Li, Z.Y. Wu, S.F. Zhang. *Inorg. Chim. Acta*, **362**, 71 (2009).
[22] S.K. Rajendran, A. Sankaralingam. *Eur. J. Med. Chem.*, **44**, 1878 (2009).
[23] Y.T. Li, W. Sun, Z.Y. Wu, Y.J. Zheng, C.W. Yan. *J. Inorg. Organomet. Polym.*, **20**, 586 (2010).
[24] Y.T. Li, W. Sun, Z.Y. Wu, C.W. Yan, Y.J. Zheng. *J. Inorg. Organomet. Polym.*, **21**, 182 (2011).
[25] H. Ojima, K. Nonoyama. *Coord. Chem. Rev.*, **92**, 85 (1998).
[26] A.R. Jose, R. Rafael, F. Juan, L. Francesc, J. Miguel, J. Yves, P.L. Michele, B. Clardette. *J. Chem. Soc., Dalton Trans.*, 3769 (1994).
[27] G.M. Sheldrick. *SHELXL-97, Program for Crystal Structure Refinement*, University of Göttingen, Germany (1997).
[28] J. Marmur. *J. Mol. Biol.*, **3**, 208 (1961).
[29] M.E. Reichmann, S.A. Rice, C.A. Thomas, P. Doty. *J. Am. Chem. Soc.*, **76**, 3047 (1954).
[30] J.B. Chaires, N. Dattagupta, D.M. Crothers. *Biochem.*, **21**, 3933 (1982).

[31] G. Cohen, H. Eisenberg. *Biopolymers*, **8**, 45 (1969).
[32] J.K. Barton, J.M. Goldberg, C.V. Kumar, N.J. Turro. *J. Am. Chem. Soc.*, **108**, 2081 (1986).
[33] G.A.V. Albada, A. Mohamadou, I. Mutikainen, U. Turpeinenc, J. Reedijk. *Acta Cryst.*, **E60**, m1160 (2004).
[34] W.J. Geary. *Coord. Chem. Rev.*, **7**, 81 (1971).
[35] N.F. Curtis. *J. Chem. Soc.*, 4109 (1963).
[36] N.F. Curtis. *J. Chem. Soc.*, 1584 (1968).
[37] R. Pascual, G.M. Carmen, L. Antonio, I.B. Javier, C. Juan, L. Francesc, J. Miguel, A. Santiago. *Inorg. Chem.*, **35**, 3741 (1996).
[38] A. Wolfe, G.H. Shimer Jr, T. Meehan. *Biochemistry*, **26**, 6392 (1987).
[39] A.I. Matesanz, P. Souza. *J. Inorg. Biochem.*, **101**, 245 (2007).
[40] R. Indumathy, S. Radhika, M. Kanthimathi, T. Weyhermuller, B.U. Nair. *J. Inorg. Biochem.*, **101**, 434 (2007).
[41] O. Stern, M. Volmer. *Z. Phy.*, **20**, 183 (1919).
[42] S. Satyanarayana, J.C. Dabrowiak, J.B. Chaires. *Biochemistry*, **31**, 9319 (1992).
[43] L. Jin, P. Yang. *J. Inorg. Biochem.*, **68**, 79 (1997).
[44] S. Satyanarayana, J.C. Dabrowiak, J.B. Chaires. *Biochemistry*, **32**, 2573 (1993).
[45] M. Jiang, Y.T. Li, Z.Y. Wu, Z.Q. Liu, X. Wu. *J. Inorg. Organomet. Polym.*, **18**, 448 (2008).